Title

Quantitative Adverse Outcome Pathway Analysis of Hatching in Zebrafish with CuO Nanoparticles

Journal

Environmental Science & Technology, 49(19)

ISSN

0013-936X 1520-5851

Authors

Muller, Erik B
Lin, Sijie
Nisbet, Roger M

Publication Date

2015-09-28

DOI

10.1021/acs.est.5b01837

Peer reviewed

Environmental Science & Technology

Article

pubs.acs.org/est

Quantitative Adverse Outcome Pathway Analysis of Hatching in Zebrafish with CuO Nanoparticles

Erik B. Muller,*[,†] Sijie Lin,[‡] and Roger M. Nisbet[§]

[†]Marine Science Institute, University of California, Santa Barbara, Santa Barbara, California 93106, United States

[‡]Center for Environmental Implications of Nanotechnology, University of California, Los Angeles, Los Angeles, California 90095, United States

[§]Department of Ecology, Evolution and Marine Biology, University of California, Santa Barbara, Santa Barbara, California 93106, United States

Supporting Information

ABSTRACT: This study develops and evaluates a mechanistic model of the hatching of zebrafish eggs that were exposed to CuO engineered nanoparticles (ENP) in a high-throughput screening system and places this model in an adverse outcome pathway (AOP) that also includes CuO ENP dissolution and Cu bioaccumulation. Cu^{2+} inhibits the proteolytic activity of Zebrafish Hatching Enzyme 1 and thereby delay or impair hatching success. This study demonstrates that noncompetitive inhibition kinetics describe the impact of dissolved Cu on hatching; it is estimated that indefinitely long exposure to 1.88 μM dissolved Cu in the environment reduces hatching enzyme activity by 50%. The complexity arising from CuO ENP dissolution and CuO ENP assisted bioaccumulation of Cu has led to apparently contradictory findings about ion versus "nano" effects on hatching. Model-mediated data analyses indicate that, relative to copper salts, CuO ENPs increase the uptake rates of Cu into the perivitelline space up to 8 times. The toxicity assessment framework in this study can be adapted to accommodate other types of toxicant, environmental samples and other aquatic oviparous species.

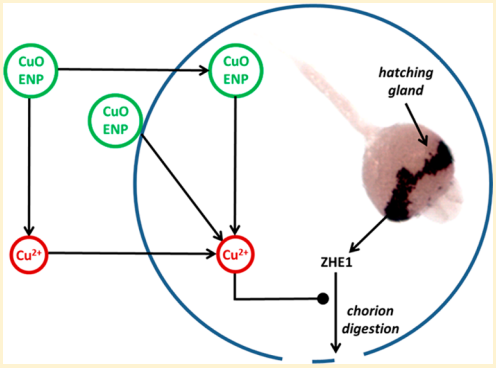

INTRODUCTION

An important task for ecotoxicology is to improve the predictive power of ecological risk assessment [see, e.g., ref 1]. The need for predictive power has been a strong impetus to develop adverse outcome pathway (AOP) analyses, which describe networks of causally linked events at different levels of biological organization,[2] and to develop general quantitative methods that summarize toxicant impact in process-based toxicity measures [see, e.g., refs 3 and 4]. Integration of these two developments into quantitative AOP approaches promises to yield powerful predictive tools for ecological risk assessment. These approaches, in which toxicity metrics relate to chemical, biological and ecological processes, eliminate or reduce the dependence of toxicity assessments on experimental design, choices of endpoint, and species of organism and chemical compound. Furthermore, quantitative AOPs open the way to using results from (semi)automated high-throughput and high-content screening tests to anticipate the impact of toxicants on processes at ecologically relevant levels of biological organization. Typically, those rapid and cost-efficient screening tests record molecular, cellular or individual responses to toxicant exposure in a dose−response manner in order to rank the hazard of a group of compounds.[5,6] Data from those screening tests could also be analyzed within a quantitative AOP framework.

The imperative need for quantitative AOP approaches has become increasingly evident due to developments in nanotechnology. The explosive growth in applications of engineered nanoparticles (ENPs) in consumer products, industry and agriculture imposes challenges to ecological risk assessment. ENPs add new dimensions of complexity to ecological risk assessment in the form of particle size and shape, which are important determinants for the potential of ENPs to cause environmental damage.[7,8] Furthermore, because many metal and metal oxide ENPs dissolve and/or speciate slowly, it is often hard to distinguish the direct toxic impact of an ENP from that of one of its constituents. To delineate the contributions of multiple factors to the toxicity profile of an ENP, quantitative methods are indispensable.

This study develops and evaluates a quantitative AOP, outlined in Figure 1, to analyze data from high-throughput screening systems that record the hatching success of zebrafish eggs exposed to ENPs.[9,10] The use of hatching success of zebrafish eggs as an endpoint is widespread in ecotoxicology [see, e.g., refs 11−18], but, to the best of our knowledge, a

Received: April 11, 2015
Revised: September 14, 2015
Accepted: September 17, 2015
Published: September 17, 2015

DOI: 10.1021/acs.est.5b01837
Environ. Sci. Technol. 2015, 49, 11817−11824

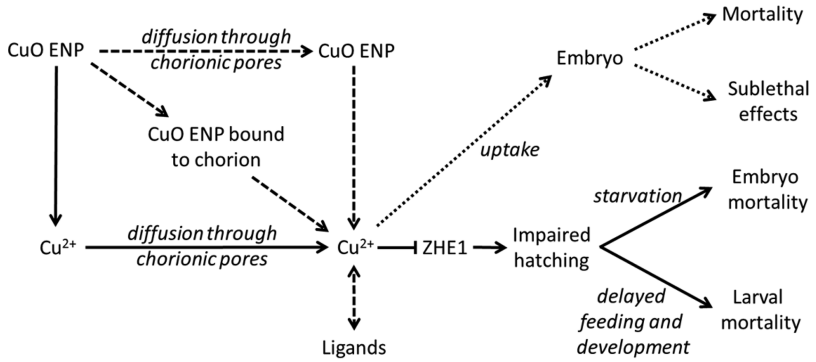

Figure 1. Mechanisms of CuO ENP toxicity. CuO ENPs shed Cu ions, which diffuse through chorionic pores into the perivitelline space, where they inhibit Zebrafish Hatching Enzyme 1 (ZHE1) and thereby impair the hatching process, which, in turn may lead to starvation conditions for embryos in unhatched eggs, and a delay in feeding in larvae (solid arrows). Tentative processes explored in this study (broken arrows) include (1) the attenuation of ZHE1 inhibition due to the binding of Cu to ligands in the perivitelline space; and (2) Cu enhanced uptake via diffusion of CuO ENPs into the perivitelline space and/or via the shedding of Cu ions from chorion bound CuO ENPs. Mechanisms for future exploration (dotted arrows) include the accumulation of Cu in embryos and subsequent toxic effects.

mechanistic hatching model is lacking. There are various toxic mechanisms that delay or prevent zebrafish eggs from hatching, such as those leading to mortality, developmental deformation and delay and those that directly impair the hatching process.[19] The latter are particularly suitable for the purpose of this study, as the mechanisms involved are relatively simple and well understood. Hatching may occur when the chorion has been sufficiently weakened by proteolytic hatching enzymes, particularly ZHE1, which are stored in gland cells before being released in the perivitelline space.[20] The activity of ZHE1, an astacin protease with zinc in its active center, is affected by transition metal ions, notably Ni^{2+}, Cu^{2+}, Cr^{2+} and Zn^{2+}.[21] Delay of hatching due to exposure to transition metal ions and ENPs containing transition metals has been observed many times [see, e.g., refs 10−12 and 15−17].

The AOP developed here specifies the events determining hatching success (see Figure 1) and describes them with quantitative models that are evaluated with both new and previously published hatching observations of zebrafish eggs exposed to $Cu(NO_3)_2$ and CuO ENPs.[9,10,15] These studies had apparently contradictory finds on the relative importance of direct "nano" effects versus toxic effects from dissolved copper. The model offers an explanation of these differences, and does so in a way that would permit predictions for future studies. The modeling approach could be easily adapted to describe the hatching process of other species.

MATERIALS AND METHODS

Experimental Procedures. Time-resolved observations of egg hatching came from two sources: a publication by Hua et al.,[15] which study will be referred to as the "Hua study", and experiments that were specifically conducted for the present study. Characteristics of exposure conditions and CuO ENPs of both sources are detailed in the Supporting Information (Tables SI-1 and SI-2, respectively).

The experimental procedures followed to collect new time-resolved observations of egg hatching, including the synthesis, handling and physicochemical characteristics of CuO nanoparticles as well as zebrafish husbandry, exposure regimen and data collection are similar to those described by Lin et al.[10] In short, CuO nanoparticles (primary size 193 ± 90 nm) were synthesized by flame spray pyrolysis as previously described.[22] Stable suspension of CuO nanoparticles in Holtfreter's medium was achieved by supplementing 100 μg/mL alginate as the dispersing agent. Wild type (AB) adult zebrafish were used for embryo spawning. Fertilized embryos at 2 h post fertilization (hpf) were robotically pick-and-placed into 96-well plates with one embryo in each well. Exposure started at 4 hpf by adding 100 μL of nanoparticle suspension into each well of the multitier plates; the nominal exposure concentrations of CuO ENP were 0, 0.02, 0.1, 0.25, 0.5, 1, 1.5, 2, 2.5 and 12.5 ppm of Cu (nominal concentrations are used to label data sets, as dissolved Cu concentrations, which are used in calculations, are dynamic quantities). Twelve embryos were used for each replicate. Bright-field high-content imaging was used to record hatching and mortality events during preceding time intervals.

Models. Processes determining the impact of CuO ENP exposure on hatching success include the dissolution of Cu, accumulation of dissolved Cu in the perivitelline space and the degradation of the chorion in the absence and presence of dissolved Cu (see Figure 1). Models for these processes are derived in the Supporting Information; this section summarizes salient features of those models and gives the model expressions that are used in fitting data on hatching success collected for the current study and those published by Hua et al.[15]

The dissolution kinetics of the CuO ENPs in our study were described by a linear model (Equation SI-1) with parameters estimated from data by Lin et al.,[9] who had used the same ENPs and experimental design as here (see Figure SI-1). The dissolved exposure Cu concentrations in the Hua study were calculated from dissolution measurements reported in the Hua study (see Table SI-3).

The accumulation of dissolved Cu in the perivitelline space was described with a one-compartment toxicokinetics model

$$\frac{dC}{dt} = k_u C_w(t) - k_e C(t) \quad (1)$$

in which C and C_w are the dissolved Cu concentrations in the perivitelline space and medium, respectively; k_u and k_e are the rate parameters for uptake and elimination, respectively. Given the small volume of the perivitelline space and low dissolved Cu concentrations therein, it is not feasible to determine those time-varying concentrations (they were measured neither in our study nor in the Hua study). Yet, the perivitelline dissolved Cu concentration, C, is assumed to determine the activity of

DOI: 10.1021/acs.est.5b01837
Environ. Sci. Technol. 2015, 49, 11817−11824

ZHE1. To get around this problem, we scale C to the ratio of the uptake and elimination rate parameters (this ratio equals the bioconcentration factor) and define the scaled dissolved Cu concentration in the perivitelline space as $c(t) \equiv k_e C(t)/k_u$ (see Supporting Information); c can be interpreted as the environmental dissolved Cu concentration that would be needed to get a particular (unscaled) steady state concentration, $C(t)$, of dissolved Cu in the perivitelline space. The benefit of this scaling is that k_u disappears as a parameter that needs to be estimated.

Ions of several transition metals, notably Ni^{2+}, Cu^{2+}, Cr^{2+} and Zn^{2+}, inhibit the activity of hatching enzyme ZHE1.[21] CuO ENPs do not inhibit enzyme activity, but Cu^{2+} ions shed from those particles do.[9] Figure SI-2 shows that the impact of Cu^{2+} on the kinetics of ZHE1 in vitro can be described with classic enzyme inhibition kinetics with ad libitum substrate

$$V(t) = \frac{C_k V_{max}}{C_k + C(t)} \tag{2}$$

in which V and V_{max} have their usual interpretation of (maximum) enzymatic rate, and C_k is the dissolved Cu concentration at which enzyme activity is reduced by 50%. This inhibition model is used to describe the impact of dissolved Cu in vivo (with scaled rather than unscaled dissolved Cu concentrations).

Hatching may occur when proteolytic enzymes have sufficiently damaged the chorion for a viable embryo to rupture it by mechanical force. This chance process was described with a hazard model. In the context of this work, a survivor is defined as an unhatched egg with a viable embryo. With hatching and death as independently occurring events, the survivor function of unhatched viable eggs, $S(t)$, is

$$S(t) = \begin{cases} S_\dagger(t) & t \le t_r \\ S_\dagger(t) e^{-k_0' c_k \int_{t_r}^{t} \frac{\tau - t_r}{c(\tau) + c_k} d\tau} & t > t_r \end{cases} \tag{3}$$

in which $S_\dagger(t)$ denotes embryo survival to time t (embryo survival is not modeled as a process here; instead, census data were used to specify $S_\dagger(t)$); k_0' specifies how fast the hatching process accelerates with increasing chorion digestion in absence of dissolved Cu; $c_k \equiv k_e C_k/k_u$ is the scaled dissolved Cu concentration in the perivitelline space at which ZHE1 activity is halved; and t_r is the time at which the embryo releases ZHE1 in the perivitelline space. In the absence of Cu toxicity and mortality in eq 3, the dynamics of egg hatching follow a Weibull distribution (see the Supporting Information), which is a standard in hazard modeling (hazard here refers to the hatching process as a "failure" to remain an egg).

Statistics. Parameters of the enzyme inhibition model were estimated by fitting eq 2 to published data while assuming additive normally distributed measurement error (see Table 1 and the Supporting Information). The hatching model as summarized in eq 3 was fitted to data collected for the present study and to data from Hua et al.[15] in order to (1) assess whether model mechanisms are plausible and sufficient in number and detail to describe the hatching dynamics of zebrafish eggs exposed to dissolved Cu and/or CuO ENPs; and (2) estimate parameter values of key processes. For this purpose, it was assumed that the number of unhatched viable eggs in a time series experiment can be seen as a trial from a multinomial distribution [cf. 23]. Let $\mathbf{y} = (y_0,...,y_n)$ be the observed number of unhatched viable eggs at successive census

Table 1. Symbols and Parameter Values

symbol	units	interpretation	value[a]	
			from data of this study	from data of Hua et al.[15]
c	μM	scaled dissolved Cu concentration in perivitelline space	variable	variable
c_k	μM	scaled inhibition constant	1.88	1.88 [0.02–6.23][b]
C_k	μM	inhibition constant	41.9[c]	41.9[c]
C_{nom}	μM	nominal concentration of Cu in ENPs	0–197	0–126
C_w	μM	dissolved Cu concentration in medium	variable	variable, see Table SI-3
k_0'	h^{-2}	hatching acceleration in absence of Cu	14.47 [3.49–56.35] 10^{-3}	4.36 [1.99–8.35] 10^{-3}[b]
k_e	h^{-1}	elimination rate of dissolved Cu from perivitelline space	0.14	0.14 [0.01 – NA][c]
k_u	h^{-1}	uptake rate of dissolved Cu from medium	3.14[e]	3.14[e]
k_u^{193}	h^{-1}	uptake rate of dissolved Cu through 193 nm CuO ENPs	23.89 [5.52–93.80]	
k_u^{25}	h^{-1}	uptake rate of dissolved Cu through 25 nm CuO ENPs		11.94 [1.83–114.42]
k_u^{50}	h^{-1}	uptake rate of dissolved Cu through 50 nm CuO ENPs		6.27 [1.37–35.94]
k_u^{100}	h^{-1}	uptake rate of dissolved Cu through 100 nm CuO ENPs		7.26 [1.70–40.88]
k_u^{400}	h^{-1}	uptake rate of dissolved Cu through 400 nm CuO ENPs		9.81 [2.44–65.22]
S	–	survivor function of unhatched viable eggs		
$S_\dagger$	–	embryo survival		
t	h	time since fertilization	variable	variable
t_r	h	start time of chorion digestion	38.63 [28.60–43.68]	45.50 [37.37–47.83][b]
V	h^{-1}	chorion digestion rate		
V_{max}	h^{-1}	maximum in vitro chorion digestion rate		

[a]With 95% confidence intervals in square brackets (values without CI are not estimated from respective data set). [b]Estimated from $Cu(NO_3)_2$ exposure data. [c]Estimated from data from enzyme kinetics assay (see Figure SI-2). [d]Upper bound confidence interval $>10^4$. [e]Implied through $k_u = k_e c_k/C_k$.

times $t_0,...,t_n$; remaining unhatched eggs after the last census will either hatch or die in the interval (t_n, ∞), i.e., $y_{n+1} = 0$. The probability for a randomly chosen egg to hatch or die between time t_{j-1} and t_j is $S_{j-1}(\boldsymbol{\theta}) - S_j(\boldsymbol{\theta})$ in which $S_j(\boldsymbol{\theta}) = S(t_j)$ is given by eq 3 and in which $\boldsymbol{\theta}$ is the vector of estimable parameters (see Table 1). Accordingly, with k replicates per treatment, the log likelihood function of the multinomial distribution is[23]

$$\ln l(\mathbf{y}|\boldsymbol{\theta}) = \sum_{i=1}^{k} \sum_{j}^{n+1} (y_{i,j-1} - y_{i,j}) \ln(S_{i,j-1}(\boldsymbol{\theta}) - S_{i,j}(\boldsymbol{\theta})) + \ln y_0! - \sum_{i=1}^{k} \sum_{j}^{n+1} \ln(y_{i,j-1} - y_{i,j})! \tag{4}$$

The best fitting parameter set $\boldsymbol{\theta}$ is the set that yields the highest value for $\ln l(\mathbf{y}|\boldsymbol{\theta})$ (to find this set, the last two terms can be ignored as these do not depend on parameter values).

Fit results were evaluated with 95% confidence intervals, which were calculated with negative log likelihood profiles. The mean absolute error, i.e., the mean absolute difference between observations and model predictions, served as a goodness-of-fit

DOI: 10.1021/acs.est.5b01837
Environ. Sci. Technol. 2015, 49, 11817–11824

measure. Model extensions, as described in the next section, were evaluated with likelihood ratio tests.

Experimental Differences between Data Sources. The time-resolved observations of hatching of unexposed and exposed eggs used to evaluate model performance came from two sources: the present study and the publication by Hua et al.[15] The experimental designs used in these two sources differ with respect to type of CuO ENPs (see Table SI-2), exposure regime (see Table SI-1), documentation thereof and observed (sub)lethal effects (as is explained elsewhere, the modeling framework developed in this paper enables the comparison of hatching observations among experimental designs). The current study used a single primary size ENPs that had been made in-house;[9,10] the Hua study involved four commercially available CuO ENPS with different primary sizes, in addition to $Cu(NO_3)_2$. Furthermore, in the present study, alginate prevented, at least partially, the ENPs from aggregating and associating with the chorion,[10] and ENPs were added only once at 4 h post fertilization (hpf). In the Hua study, measures to prevent aggregation were not applied and medium was refreshed every 24 h with initial exposure starting at 24 hpf. Accordingly, exposure regimes differed between the two studies (see the Supporting Information for reconstructions of exposure regimes). In addition, all embryos in the present study remained viable and did not show signs of sublethal effects (besides deformation due to space limitation in late hatchers), whereas mortality in the Hua study was considerable, notably at the higher exposure levels. Mortality in the Hua study is accounted for by excluding exposure levels at which (nearly) all embryos died before hatching and by using mortality data in the calculation of model predictions.

RESULTS AND DISCUSSION

The quantitative AOP approach of this study principally aims at assessing the impact of CuO ENPs on hatching of zebrafish eggs and, secondarily, at synthesizing apparently contradictory finds on the relative importance of direct "nano" effects versus toxic effects from dissolved copper. The AOP is quantified through process-based models describing fish egg hatching dynamics, toxicokinetics, toxicodynamics, including enzyme inhibition kinetics, and through phenomenological descriptions of CuO ENP dissolution. Because the models for enzyme inhibition kinetics and CuO ENP dissolution play a subsidiary role, these models are evaluated and parametrized with previously published data[9,10,15] in the Supporting Information. New time-resolved observations of hatching of unexposed eggs are used to evaluate the model describing egg hatching dynamics (see Figure 2); this evaluation is amended with similar data published by Hua et al.,[15] whose study also provided time-resolved hatching observations to evaluate the toxicity of dissolved Cu (see Figure 3) and of CuO ENPs (see Figure 4) on hatching dynamics. Furthermore, the modeling framework is also evaluated with new time-resolved observations of hatching of eggs exposed to a relatively wide range of CuO ENP concentrations (see Figure 5). This section concludes with a discussion about potential model extensions that could widen the applicability of the approach and the need to reduce the dependency of toxicity assessment measures on experimental design and duration.

From the time-resolved observations and model fits of hatching of unexposed eggs of the present and Hua study, two conclusions are immediately apparent (see Figure 2). First, the hatching dynamics of eggs in the current study differ considerably from those in the Hua study. Although both studies use eggs from wild type zebrafish and assay conditions seem comparable (the temperature in our experiments is 0.5 °C higher than that in the Hua study), eggs in the present study start to hatch earlier and complete hatching in a narrower time frame than those of Hua. These observations are mirrored by the estimates of parameter values: chorion digestion in this study starts nearly 1 h earlier and then accelerates more than 1 order of magnitude faster than in that of Hua (see legend to Figure 2). Possibly, the embryos in the Hua study develop a little slower and produce considerably less hatching enzymes or

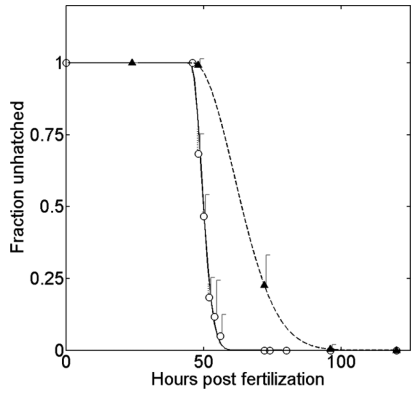

Figure 2. Hatching results and model fits eq 3 in the controls of current study (open circles, solid line) and of the one by Hua et al.[15] (triangles, broken line). The data and error bars represent the mean fraction and standard deviation of unhatched viable eggs of 5 replicates of 12 eggs (current study) or 15 replicates of 16 eggs (Hua study). Estimates (with 95% confidence intervals) of the onset of chorion digestion, t_r, and the hatching acceleration, k_0', are 45.2 (44.1−45.9) hpf and 0.063 (0.04−0.09) h^{-2} (current study; mean absolute error of model predictions is 0.03), and 46.1 (43.1−47.7) hpf and 0.004 (0.003−0.006) h^{-2} (Hua study; mean absolute error is 0.02), respectively.

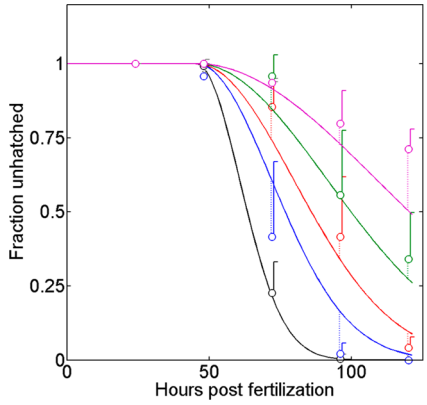

Figure 3. Course of the mean fraction of unhatched viable eggs exposed to $Cu(NO_3)_2$. From bottom to top, curves represent model fits to data relating to nominal Cu concentrations increasing from 0 (black), 0.25 (blue), 0.5 (red), 1 (green) and 2 (purple) ppm; until approximately 50 hpf data and model fits at all exposure levels are overlapping (available data from 4 and 8 ppm of CuO are excluded, as nearly all embryos died before hatching). Model fits are based on dissolved Cu concentrations in the medium and perivitelline space (with eq 1 and 3; see text). Dotted lines connect data to corresponding model fits. Vertical lines represent standard deviations of 15 (control) or 3 (all exposure levels) replicates of the means of 16 eggs; the mean absolute error of model predictions is 0.04. Parameter estimates are listed in Table 1. Data from Hua et al.[15]

DOI: 10.1021/acs.est.5b01837
Environ. Sci. Technol. 2015, 49, 11817−11824

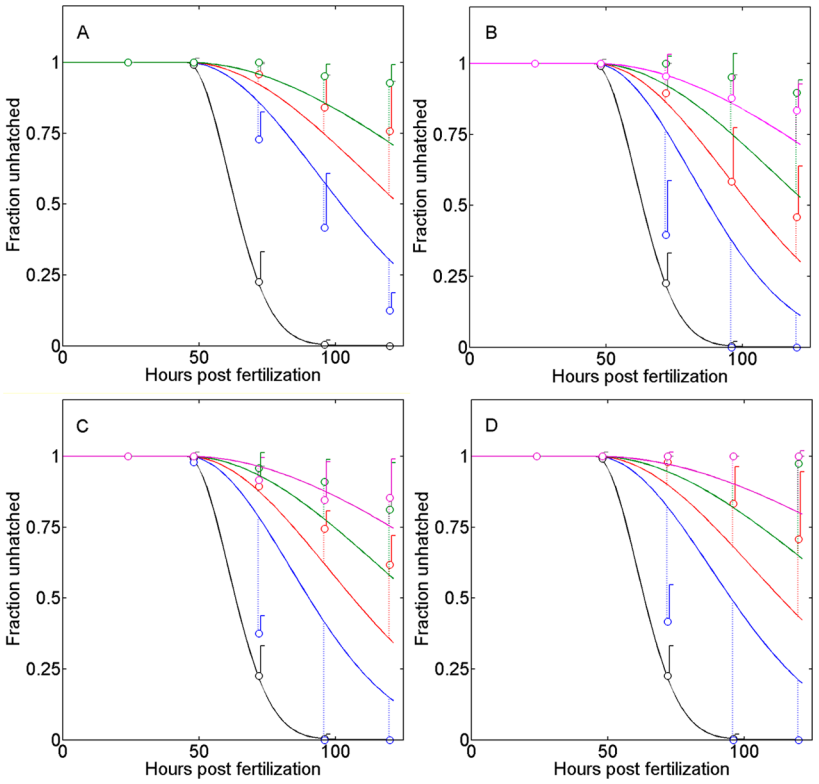

Figure 4. Course of the mean fraction of unhatched viable eggs (circles) exposed to CuO ENPs with primary diameter of 25 nm (A), 50 nm (B), 100 nm (C) or 400 nm (D). From bottom to top, curves represent model fits to data relating to nominal Cu concentrations increasing from 0 (black), 0.25 (blue). 0.5 (red), 1 (green) and 2 (purple) ppm; until approximately 50 hpf data and model fits at all exposure levels are overlapping (available data from 4 and 8 ppm of all primary size ENPs and 2 ppm 25 nm ENPs are excluded, because all or nearly all eggs died before hatching). Model fits are based on dissolved Cu concentrations in the medium and perivitelline space (with eqs 1 and 3; see text). Dotted lines connect data to corresponding model fits. Vertical lines represent standard deviations of 15 (control) or 3 (all exposure levels) replicates of the means of 16 eggs; the mean absolute error of model predictions is 0.04 (A), 0.06 (B), 0.04 (C) and 0.10 (D). Parameter estimates are listed in Table 1. Data from Hua et al.[15]

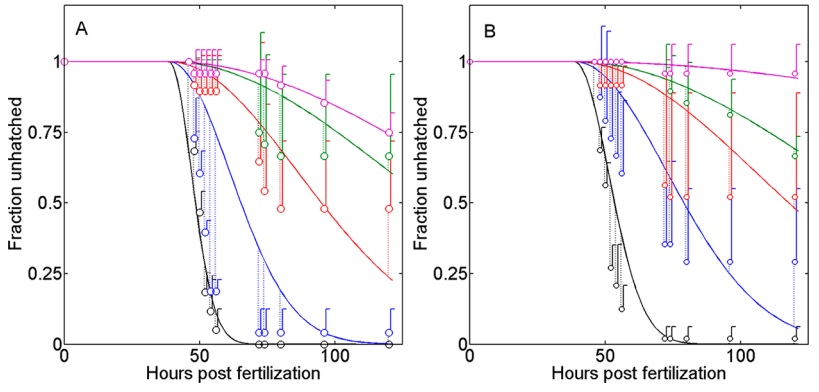

Figure 5. Course of the mean fraction of unhatched viable eggs (circles) exposed to CuO ENPs at nominal concentrations of 0 (black), 0.1 (blue), 0.5 (red), 1.5 (green) and 2.5 ppm (purple) Cu (A) and 0.02 (black), 0.25 (blue), 1 (red), 2 (green) and 12.5 (purple) ppm of Cu (B); note exposure levels alternate between the panels. From bottom to top, curves represent model fits to data relating to increasing nominal CuO ENP concentrations; yet, model fits are based on dissolved Cu concentrations in the medium and perivitelline space (with eqs 1 and 3; see text); until approximately 50 hpf data and model fits at all exposure levels are overlapping. Dotted lines connect data to corresponding model fits. Vertical lines represent standard deviations of 5 (control), 6 (12.5 ppm) or 4 (all other exposure levels) replicates of the means of 12 eggs; the mean absolute error of model predictions is 0.11. Parameter estimates are listed in Table 1.

have stronger chorions than those in the present study. Second, the model (eq 3 with $c = 0$) fits time-resolved observations of the hatching of viable unexposed eggs very well. The mean absolute error is 0.02 for our data and 0.03 for Hua's data, implying that individual observations deviate on average 0.02–0.03 from model predictions. Thus, the egg hatching model is a suitable baseline for the assessment of dissolved Cu and CuO ENP toxicity on egg hatching dynamics.

The impact of exposure to dissolved $Cu(NO_3)_2$ is evident from the widening interval of hatching times with increasing exposure levels (see Figure 3). Exposure to dissolved Cu slows down the hatching process. This trend is predicted by the

DOI: 10.1021/acs.est.5b01837
Environ. Sci. Technol. 2015, 49, 11817–11824

model through a decline in hatching acceleration due to the inhibition of ZHE1 by dissolved Cu accumulated in the perivitelline space. The activity of ZHE1, and hence the hatching acceleration, are reduced by 50% when eggs are exposed to 1.88 μM dissolved Cu in the environment, provided steady state dissolved Cu concentrations in the perivitelline space are established before the release of ZHE1. From a practical point of view, this condition appears to have been met, as estimates of the toxicant exchange rate parameters (see Table 1) suggest that dissolved Cu concentrations in the perivitelline space had approached 95% of their ultimate steady state values at the time of ZHE1 release. However, it should be noted that, due to the lack of perivitelline dissolved Cu measurements, the precision of these estimates is low, as is illustrated by the wide confidence interval for the estimate of the elimination rate parameter. Furthermore, the data suggest that the onset of the hatching process is not delayed due to dissolved Cu exposure. In accordance, the estimated value of t_r, i.e., the start time of chorion digestion (see Table 1), does not differ significantly from that estimated from the control data (see legend to Figure 2).

The model describes the observed trends in hatching of eggs exposed to dissolved Cu generally well (mean absolute error is 0.10) with two notable exceptions (see Figure 3). At the lowest exposure level, the model predicts a stronger impact than seems warranted by the data, whereas it underestimates the response to the highest exposure concentration. This suggests that there is a no-effect concentration,[3,24] i.e., a threshold concentration of dissolved Cu in the perivitelline space below which ZHE1 inhibition does not occur, possibly due to the presence of Cu^{2+} binding ligands in the perivitelline space (note that such a threshold is absent in vitro, see Figure SI-2). The no-effect concentration, c_0, can be estimated by substituting $(c(t) - c_0)_+$ for $c(t)$ in eq 3, which visually improves the model fits at the lowest and highest exposure concentrations substantially while only marginally changing those of others (see Figure SI-3A). However, the estimated value for c_0, 3.27 μM, does not differ significantly from 0 at the 95% level in a log likelihood ratio test (see Figure SI-3B). This indicates that a proper assessment of the no-effect concentration requires hatching observations at more, relatively low exposure levels than used in these experiments.

Exposure to CuO ENPs has an impact that is qualitatively similar to that of dissolved Cu exposure. The interval of hatching times widens with increasing exposure levels (see Figure 4 and 5) and, accordingly, decreasing ZHE1 activity. In addition, at higher exposure levels in the present study, the hatching process seems to stall, which the model explains as the result of continuing perivitelline Cu accumulation due to ongoing CuO ENPs dissolution in the medium. However, because only a fraction of CuO ENPs dissolved in each exposure medium (see Figure SI-1 and Table SI-3), the magnitude of impact due to CuO ENP exposure is higher than should be expected on the basis of dissolved Cu in exposure media alone, as Hua et al. have also noted.[15] Accordingly, with parameter values estimated from hatching observations of eggs exposed to dissolved $Cu(NO_3)_2$, the model projects hatching trajectories of eggs exposed to CuO ENPs that grossly discount observed impacts if only dissolved Cu in the medium is considered (results not shown). Because CuO ENPs do not directly reduce the activity of ZHE1, but only through shedding of Cu^{2+},[9] the cause of this ENP enhanced Cu toxicity is most likely due to an increase in dissolved Cu accumulation in the perivitelline space, as was also proposed by Hua et al.[15] CuO ENPs used in the present study stain the outside of eggs, indicating that they have a high affinity to bind to or associate with the chorion. Possibly, this binding diminishes the diffusion barrier between bulk and chorion and thereby facilitates the diffusion of dissolved Cu and/or small CuO ENPS through chorionic pores.[11]

To investigate the likeliness of ENP enhanced Cu uptake as explanatory mechanism, we analyze the hatching results of both studies while assuming an additional diffusive Cu uptake pathway operating at a rate proportional to the nominal CuO ENP concentration, C_{nom}. This means that uptake in eq 3 becomes $k_u C_w + k_u^* C_{nom}$, in which k_u^* is the rate constant specifying Cu uptake mediated by ENPs with primary size *.

With the toxicokinetic and toxicodynamic parameter values of the $Cu(NO_3)_2$ data set, this modification vastly improves the ability of the model to describe the data of both studies, although, as with exposure to $Cu(NO_3)_2$, the model consistently overestimates impact at the lower CuO ENP exposure levels observed in both studies (see blue model curves fitted to data in all panels of Figures 4 and 5), and underestimates impact at the higher exposure levels observed in the Hua study (see green and purple model curves fitted to data in all panels of Figure 4). Indeed, fits visually improve when considering a nonzero no-effect concentration (results not shown), but it is likely that approximation errors made in the reconstruction of medium dissolved Cu concentrations also contributed to these estimation biases. Estimates for k_u^* indicate that, at equal dissolved Cu and CuO ENP concentrations, the rate of uptake of Cu via CuO ENPs is 2 to 4 times higher than that through dissolved Cu in the Hua study and 7 to 8 times higher in the present study (see Table 1).

The difference between those uptake enhancement factors may in part be attributed to the speciation behavior of dissolved Cu in exposure medium and perivitelline space. The ionic composition of exposure medium differed between studies (see Table SI-1). Furthermore, the addition of alginate to the ENP solutions in the experiments of the present study stabilized the ENPs. Being a polyanionic polymer, alginate increases the negative value of the surface charge of CuO ENPs, thereby enhancing electro-repulsion among CuO ENPs and, consequently, reducing the formation of aggregates and maintaining a relatively large average surface to volume ratio of ENPs[10] (this stabilizing effect may also in part explain why the model fits to data of the present study show less bias than those of the Hua study). This factor appears not to depend on the primary size of ENPs, which suggests that ENP diffusion through chorionic pores is an unlikely explanatory mechanism, as the diameter of chorionic pores is smaller than the size of the larger ENPs in the Hua study.[15] This suggests that CuO ENPs enhance the uptake of Cu through diminishing the diffusion barrier between bulk and chorion.

The results and model analyses above show that (1) a standard hazard model represents the dynamics of egg hatching very well; (2) a simple, routine model of enzyme inhibition kinetics effectively serves as the basis of a model describing the impact of dissolved Cu on hatching; and (3) relative to dissolved Cu, CuO ENPs have a strong negative impact on hatching, which is likely due to enhanced Cu uptake via CuO ENPs. It should be noted that these conclusions stem from comparative analyses of data from experiments with very different exposure regimes. In the modeling framework, the strong impact of exposure regime on hatching is accounted for

DOI: 10.1021/acs.est.5b01837
Environ. Sci. Technol. 2015, 49, 11817−11824

by generalizing the environmental exposure levels of various Cu containing compounds into a single measure, i.e., the dissolved Cu concentration in the perivitelline space (which is assumed to determine the activity of ZHE1 and, hence, the dynamics of hatching). From an experimental point of view, the dissolved Cu concentration in the perivitelline space appears to be a remote quantity, as it would take an unjustifiably large number of eggs and prohibitively large amount of CuO ENPs to document its dynamics. However, with the aid of models, it can be dealt with using an implicit quantity whose dynamics are governed by (measured) environmental dissolved Cu concentrations and time-resolved hatching observations.

Furthermore, it should be emphasized that the comparative analyses of this study critically depended on the availability of time-resolved data, as single time-point measurements inherently lack information about dynamic processes (just as it would be impossible to reconstruct a movie from a single snapshot). Endpoints in ecotoxicological risk assessment studies are generally subject to dynamic processes, but notably high-throughput screening methods often yield dose−response curves for single time points only. If those methods were adapted to generate time-resolved data, they would substantially gain in delivering predictive power.

The design and quantitative analysis of the AOP in this study is relatively simple as the mechanisms involved are few and, with the exception of nanoparticle behavior, well understood. On the downside, the assessment method of this study seems limited to toxicants with hatching enzymes as primary targets, i.e., to certain transition metals. However, the current AOP can be adapted to accommodate other types of toxicants that affect the hatching process of potentially a wide variety of fish species (and, possibly, other aquatic oviparous vertebrates and invertebrates). Within the range of exposure levels we used in this study, CuO ENPs appear to only affect the hatching process. We observed spinal deformations in some CuO ENP exposed embryos that, given their size and stage of development, ought to have hatched, but attribute this effect to the embryos' confinement to a space that was too small for normal spinal growth. Besides this deformation likely due to failed hatching, no impact of CuO ENP exposure on development or growth was detected. Accordingly, a distinguishing feature in hatching profiles observed in the data collected for this study as well of those of Hua is the apparently invariant timing of hatching initiation, regardless of exposure level of dissolved Cu.

In contrast, toxicity mechanisms other than ZHE1 inhibition are likely to affect the timing of hatching initiation. For example, Zhou et al.[18] have shown that cartap, a neurotoxic insecticide, likely impairs the glandular release of hatching enzymes in zebrafish, which release is under neurological control. This type of toxic impact translates into an increase in t_r in the current AOP (see eq 3) and may be quantified with the process-based model developed by Jager and Kooijman,[25] who have described the impact of organophosphorus insecticides on receptor kinetics of insects. Furthermore, toxicity mechanisms affecting hatching indirectly, e.g., through a delay in embryonic development, may be quantified by incorporating the current AOP in the DEBtox framework,[1,3] in which the bioenergetic implications of toxicant effects are quantified. Finally, mortality affects the survivor function of the current AOP (see eq 1). Our aim is to account for mortality with models describing the accumulation of damage due to chemical insult that are currently being developed by us and co-workers.

High-throughput screening systems, such as the one used in this study, are very efficient tools to determine relatively short-term impacts of toxicant exposure on small life forms. With quantitative AOPs, those impacts can be translated to toxicity assessment measures relating to chronic exposure. For example, our model analysis shows that indefinitely long exposure to 1.88 μM dissolved Cu in the environment reduces hatching enzyme activity with 50% (see Table 1) and reduces the acceleration of the hatching process accordingly. This potential to translate results from relatively short experiments to long-term effects is highly relevant for ecological risk assessment, as exposure to contaminants in the environment often spans multiple generations, whereas a delay in hatching can severely reduce subsequent survival. Furthermore, processes determining the fate of CuO ENPs in natural environments, such as dissolution, aggregation and sedimentation, are relatively slow and strongly depend on environmental conditions, such as pH, salinity and ligand content.[26] With our quantitative AOP, effects of these processes on hatching can be delineated from the impact of dissolved Cu. Quantitative AOPs can diminish the impact of choices about experimental design in ecological risk assessment and yield toxicity assessment measures with an improved potential to predict impact at higher levels of biological organization.

■ ASSOCIATED CONTENT

Supporting Information

The Supporting Information is available free of charge on the ACS Publications website at DOI: 10.1021/acs.est.5b01837.

Exposure conditions (Table SI-1), characteristics of CuO ENPs (Table SI-2), and reconstructions of dissolved Cu exposure concentrations and model derivations. Figure SI-1 and Table SI-3 justify these reconstructions. Figure SI-2 shows data and model fits and parameter estimates about ZHE1 inhibition by Cu. Figure SI-3 illustrates the improvement of model fit to the hatching dynamics of eggs exposed to dissolved Cu by including a no-effect concentration in the modeling framework (PDF).

■ AUTHOR INFORMATION

Corresponding Author

*E. B. Muller. E-mail: erik.muller@lifesci.ucsb.edu.

Notes

The authors declare no competing financial interest.

■ ACKNOWLEDGMENTS

We thank Tjalling Jager for sharing Matlab code for the estimation of parameter values, Jing Hua for providing data files, Linda Dong and William Ueng for the support on zebrafish care and spawning and Suman Pokhrel and Lutz Mädler for providing CuO nanoparticles. We are also indebted to Tin Klanjscek and Gary Cherr for valuable discussions. We are also indebted to the three anonymous reviewers, whose suggestions and comments led to substantial improvements in the paper. This research was supported by the U.S. National Science Foundation and the U.S. Environmental Protection Agency under Cooperative Agreement Number DBI-1266377. Any opinions, findings, and conclusions or recommendations expressed in this material are those of the authors and do not necessarily reflect the views of the National Science Foundation or the U.S. Environmental Protection Agency. This work has

DOI: 10.1021/acs.est.5b01837
Environ. Sci. Technol. 2015, 49, 11817−11824

not been subjected to EPA review and no official endorsement should be inferred.

REFERENCES

(1) Forbes, V. E.; Calow, P. Developing predictive systems models to address complexity and relevance for ecological risk assessment. *Integr. Environ. Assess. Manage.* **2013**, *9* (3), e75−e80.

(2) Ankley, G. T.; Bennett, R. S.; Erickson, R. J.; Hoff, D. J.; Hornung, M. W.; Johnson, R. D.; Mount, D. R.; Nichols, J. W.; Russom, C. L.; Schmieder, P. K.; Serrrano, J. A.; Tietge, J. E.; Villeneuve, D. L. Adverse outcome pathways: a conceptual framework to support ecotoxicology research and risk assessment. *Environ. Toxicol. Chem.* **2010**, *29* (3), 730−741.

(3) Jager, T. Some Good Reasons to Ban ECx and Related Concepts in Ecotoxicology. *Environ. Sci. Technol.* **2011**, *45* (19), 8180−8181.

(4) Muller, E. B.; Nisbet, R. M.; Berkley, H. A. Sublethal toxicant effects with dynamic energy budget theory: model formulation. *Ecotoxicology* **2010**, *19* (1), 48−60.

(5) George, S.; Xia, T. A.; Rallo, R.; Zhao, Y.; Ji, Z. X.; Lin, S. J.; Wang, X.; Zhang, H. Y.; France, B.; Schoenfeld, D.; Damoiseaux, R.; Liu, R.; Lin, S.; Bradley, K. A.; Cohen, Y.; Nel, A. E. Use of a High-Throughput Screening Approach Coupled with In Vivo Zebrafish Embryo Screening To Develop Hazard Ranking for Engineered Nanomaterials. *ACS Nano* **2011**, *5* (3), 1805−1817.

(6) Nel, A.; Xia, T.; Meng, H.; Wang, X.; Lin, S. J.; Ji, Z. X.; Zhang, H. Y. Nanomaterial Toxicity Testing in the 21st Century: Use of a Predictive Toxicological Approach and High-Throughput Screening. *Acc. Chem. Res.* **2013**, *46* (3), 607−621.

(7) Xia, T.; Malasarn, D.; Lin, S. J.; Ji, Z. X.; Zhang, H. Y.; Miller, R. J.; Keller, A. A.; Nisbet, R. M.; Harthorn, B. H.; Godwin, H. A.; Lenihan, H. S.; Liu, R.; Gardea-Torresdey, J.; Cohen, Y.; Madler, L.; Holden, P. A.; Zink, J. I.; Nel, A. E. Implementation of a Multidisciplinary Approach to Solve Complex Nano EHS Problems by the UC Center for the Environmental Implications of Nanotechnology. *Small* **2013**, *9* (9−10), 1428−1443.

(8) Zhu, M. T.; Nie, G. J.; Meng, H.; Xia, T.; Nel, A.; Zhao, Y. L. Physicochemical Properties Determine Nanomaterial Cellular Uptake, Transport, and Fate. *Acc. Chem. Res.* **2013**, *46* (3), 622−631.

(9) Lin, S. J.; Zhao, Y.; Ji, Z. X.; Ear, J.; Chang, C. H.; Zhang, H. Y.; Low-Kam, C.; Yamada, K.; Meng, H.; Wang, X.; Liu, R.; Pokhrel, S.; Madler, L.; Damoiseaux, R.; Xia, T.; Godwin, H. A.; Lin, S.; Nel, A. E. Zebrafish High-Throughput Screening to Study the Impact of Dissolvable Metal Oxide Nanoparticles on the Hatching Enzyme, ZHE1. *Small* **2013**, *9* (9−10), 1776−1785.

(10) Lin, S. J.; Zhao, Y.; Xia, T.; Meng, H.; Ji, Z. X.; Liu, R.; George, S.; Xiong, S. J.; Wang, X.; Zhang, H. Y.; Pokhrel, S.; Madler, L.; Damoiseaux, R.; Lin, S.; Nel, A. E. High Content Screening in Zebrafish Speeds up Hazard Ranking of Transition Metal Oxide Nanoparticles. *ACS Nano* **2011**, *5* (9), 7284−7295.

(11) Bai, W.; Tian, W. J.; Zhang, Z. Y.; He, X. A.; Ma, Y. H.; Liu, N. Q.; Chai, Z. F. Effects of Copper Nanoparticles on the Development of Zebrafish Embryos. *J. Nanosci. Nanotechnol.* **2010**, *10* (12), 8670−8676.

(12) Dave, G.; Xiu, R. Q. Toxicity of mercury, copper, nickel, lead, and cobalt to embryos and larvae of zebrafish, brachydanio rerio. *Arch. Environ. Contam. Toxicol.* **1991**, *21* (1), 126−134.

(13) Hernandez, P. P.; Undurraga, C.; Gallardo, V. E.; Mackenzie, N.; Allende, M. L.; Reyes, A. E. Sublethal concentrations of waterborne copper induce cellular stress and cell death in zebrafish embryos and larvae. *Biological Research* **2011**, *44* (1), 7−15.

(14) Hill, A. J.; Teraoka, H.; Heideman, W.; Peterson, R. E. Zebrafish as a model vertebrate for investigating chemical toxicity. *Toxicol. Sci.* **2005**, *86* (1), 6−19.

(15) Hua, J.; Vijver, M. G.; Ahmad, F.; Richardson, M. K.; Peijnenburg, W. Toxicity of different-sized copper nano- and submicron particles and their shed copper ions to zebrafish embryos. *Environ. Toxicol. Chem.* **2014**, *33* (8), 1774−1782.

(16) Johnson, A.; Carew, E.; Sloman, K. A. The effects of copper on the morphological and functional development of zebrafish embryos. *Aquat. Toxicol.* **2007**, *84* (4), 431−438.

(17) Palmer, F. B.; Butler, C. A.; Timperley, M. H.; Evans, C. W. Toxicity to embryo and adult zebrafish of copper complexes with two malonic acids as models for dissolved organic matter. *Environ. Toxicol. Chem.* **1998**, *17* (8), 1538−1545.

(18) Zhou, S. L.; Dong, Q. X.; Li, S. N.; Guo, J. F.; Wang, X. X.; Zhu, G. N. A. Developmental toxicity of cartap on zebrafish embryos. *Aquat. Toxicol.* **2009**, *95* (4), 339−346.

(19) Jezierska, B.; Lugowska, K.; Witeska, M. The effects of heavy metals on embryonic development of fish (a review). *Fish Physiol. Biochem.* **2009**, *35* (4), 625−640.

(20) Inohaya, K.; Yasumasu, S.; Araki, K.; Naruse, K.; Yamazaki, K.; Yasumasu, I.; Iuchi, I.; Yamagami, K. Species-dependent migration of fish hatching gland cells that commonly express astacin-like proteases in common. *Dev., Growth Differ.* **1997**, *39* (2), 191−197.

(21) Gomisruth, F. X.; Grams, F.; Yiallouros, I.; Nar, H.; Kusthardt, U.; Zwilling, R.; Bode, W.; Stocker, W. Crystal-structures, spectroscopic features, and catalytic properties of cobalt(II), copper(II), nickel(II), and mercury(II) derivatives of the zinc endopeptidase astacin - a correlation of structure and proteolytic activity. *J. Biol. Chem.* **1994**, *269* (25), 17111−17117.

(22) Teoh, W. Y.; Amal, R.; Madler, L. Flame spray pyrolysis: An enabling technology for nanoparticles design and fabrication. *Nanoscale* **2010**, *2* (8), 1324−1347.

(23) Jager, T.; Albert, C.; Preuss, T. G.; Ashauer, R. General Unified Threshold Model of Survival - a Toxicokinetic-Toxicodynamic Framework for Ecotoxicology. *Environ. Sci. Technol.* **2011**, *45* (7), 2529−2540.

(24) Kooijman, S. A. L. M.; Bedaux, J. J. M.; Slob, W. No-effect concentration as a basis for ecological risk assessment. *Risk Anal.* **1996**, *16* (4), 445−447.

(25) Jager, T.; Kooijman, S. A. L. M. Modeling receptor kinetics in the analysis of survival data for organophosphorus pesticides. *Environ. Sci. Technol.* **2005**, *39* (21), 8307−8314.

(26) Adeleye, A. S.; Conway, J. R.; Perez, T.; Rutten, P.; Keller, A. A. Influence of Extracellular Polymeric Substances on the Long-Term Fate, Dissolution, and Speciation of Copper-Based Nanoparticles. *Environ. Sci. Technol.* **2014**, *48* (21), 12561−12568.

DOI: 10.1021/acs.est.5b01837
Environ. Sci. Technol. 2015, 49, 11817−11824

SUPPLEMENTAL INFORMATION
FOR
QUANTITATIVE ADVERSE OUTCOME PATHWAY ANALYSIS OF HATCHING IN ZEBRAFISH WITH CuO NANOPARTICLES

Erik B. Muller[1,*], Sijie Lin[2], Roger M. Nisbet[3]

[1]Marine Science Institute, University of California, Santa Barbara, CA 93106

[2]Center for Environmental Implications of Nanotechnology, University of California, Los Angeles, Los Angeles, CA 90095

[3]Department of Ecology, Evolution and Marine Biology, University of California, Santa Barbara, CA 93106

[*]Corresponding author erik.muller@lifesci.ucsb.edu

Table of Contents

I. Exposure conditions and CuO ENP characteristics

Table SI-1. Exposure conditions.

	This study[a]	Hua *et al.*
Embryo type	Wild type AB strain	Wild type AB strain
Concentration of Cu particles and dissolved Cu	0.02 – 12.5 ppm	0.25 – 8 ppm
Exposure starting time	4 hpf	24 hpf
Exposure duration	5 days	4 days
Exposure medium refreshment interval	none	daily
Exposure temperature	28.5°C	28 °C
Toxicity endpoint	Percent hatching and survival	Percent hatching and survival
Exposure medium	Holtfreter's medium with 100 ppm alginate	0.021% Instant Ocean® [b] salt in Milli-Q water
Major Cations	60 mM Na^+, 0.6 mM K^+, 0.7 mM Ca^{2+}	2.8 mM Na^+, 56 µM K^+, 0.31 mM Mg^{2+}, 56 µM Ca^{2+}
Major Anions	60 mM Cl^-, 2 mM HCO_3^-	3.1 mM Cl^-, 0.14 mM SO_4^{2-}, 11 µM TCO_2[c]
Exposure medium pH	7.0	6.2-6.9

[a] Same as Lin *et al.* [1]

[b] Total organic carbon < 100 ppt

[c] Total dissolved inorganic carbon

Table SI-2. CuO ENP characteristics.

	This study[a]	Hua *et al.*			
Primary size (nm)	18	25	50	100	400
Manufacturer	In house	IoLiTec	IoLiTec	IoLiTec	NanoAmor
Purity (%)	100.0	99.9	99.5	99.9	99
Preparation method	15 minute sonication	10 minute sonication			
Hydrodynamic size after 24 h (nm)	284	536 - 803 [b]	345 - 896 [b]	578 - 647 [b]	435 - 1683 [b]
Zeta potential after 24 h (mV)	-27.2	-20.5 - -5.6[b]	-8.2 - +3.2[b]	-16.3 - -8.1[b]	-4.9 - -22.4[b]

[a] Specifications from as Lin *et al.* [1]

[b]Varies depending on nominal concentration; range given for 1 ppm and 8 ppm Cu

II. Reconstruction of dissolved medium Cu concentrations

Ideally, analyses of hatching data are informed by time resolved data specifying medium and perivitelline Cu concentrations at each exposure regime. Unfortunately, such data are not available. Therefore, it is necessary to reconstruct those concentrations from published data and additional assumptions. We need separate reconstructions for each data source, i.e. the experiments of the present paper and those of Hua *et al.* [2], as exposure regimes differed between the two sets of experiments.

For the reconstruction of exposure regimes in our current study, we use published data from Lin *et al.* [1], who, over a period of 48 h, followed the dissolution of the same CuO ENPs at similar experimental conditions as in our current study but at a higher concentration (0.79 mM Cu versus nominal exposure concentrations ranging from 0 to 0.2 mM). Assuming a linear increase in the dissolved Cu concentration after the rapid initial dissolution of loosely associated Cu (see Figure SI-1) and dissolution dynamics that scale approximately linearly with the nominal concentration, C_{nom}, we describe exposure after ENP addition at 4 hours post fertilization (4 hpf) in our experiments with

$$C_w(t) = \begin{cases} 0 & t \le 4 \\ p_1 C_{nom}(t-4) + p_2 C_{nom} & t > 4 \end{cases} \qquad \text{(SI.1)}$$

in which C_w is the dissolved Cu concentration in the medium, and p_1 and p_2 are regression coefficients estimated from the data in Figure SI-1.

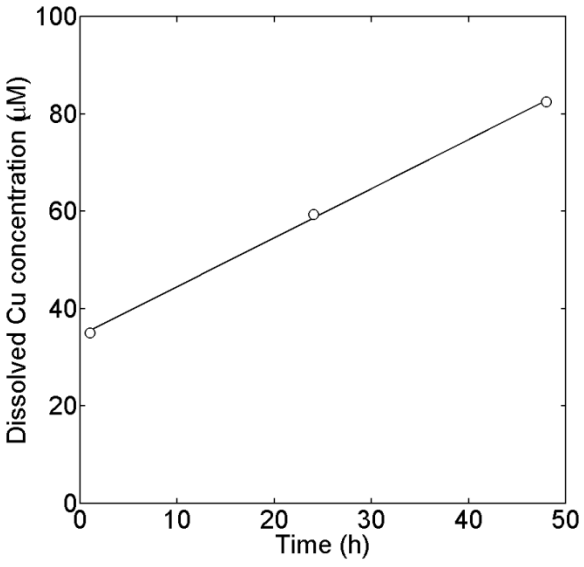

Figure SI-1. Dissolution kinetics of CuO ENP with a nominal Cu concentration of 50 ppm (0.79 mM) in Cu^{2+}-free Holtfreter's medium (data from Lin *et al.* [1]; dissolved Cu concentrations were measured with inductively coupled plasma mass spectrometry). As is indicated by the apparent initial Cu^{2+} concentration of 34.4 µM, a fraction of the nanoparticles dissolves rapidly; about 4% has dissolved within 1 hour. Subsequently, dissolution proceeds at a much lower rate (Cu^{2+} concentration increases with 1.01 µM h^{-1}); after 48 hours, about 11% of the CuO ENPs has dissolved, indicating that less than a fifth of the CuO ENPs dissolves in the 116 hour period during which eggs are exposed in screening experiments (data fitted with Equation SI.1; normalized to the nominal concentration, the dissolution rate is 1.28. 10^{-3} h^{-1} and the fraction of instantly dissolved Cu is 0.044; r^2=0.9993) .

For the reconstruction of exposure regimes in the study of Hua *et al.* [2], we use their dissolution measurements, which include dissolved Cu concentrations for a subset of nominal exposure CuO ENP concentrations (i.e. 1, 2 and 8 ppm Cu of each of their four primary size ENPs) measured 24 hours after the addition of CuO ENPs to exposure medium (without eggs). In order to reconstruct the exposure concentrations of dissolved Cu at all ENP nominal concentrations, we make two assumptions. First, the measured Cu concentrations were quickly established after the addition of ENP stock solutions and did not change significantly thereafter. This assumption is reasonable as a fraction of the ions in CuO ENPs generally dissolves rapidly, while subsequent metal ion shedding is relatively slow [3]. This occurred in the experiments of Lin *et al.* [1], as explained above, and likely also happened with the ENPs under consideration (Hua, pers. comm.). Second, we assume that the dissolved Cu concentrations that were measured 24 h after the addition of CuO ENPs of a particular size class, $C_w(24)$, can be described as a function of the nominal CuO ENP concentration with the phenomenological expression

$$C_w(24) = C_\infty(24) - \frac{1}{p_3 C_{nom} + p_4} \qquad \text{(SI.2)}$$

in which $C_\infty(24)$ is the dissolved Cu concentration 24 h after the addition of a very high nominal ENP concentrations, and p_3 and p_4 are regression parameters (parameter values differ among ENP size classes). This expression fits the data well, as differences between measured and reconstructed dissolved Cu concentrations are small (see Table SI-1).

Table SI-1. Dissolved Cu concentrations in the experiments of Hua *et al.* [2]

Nominal [Cu2+]	Dissolved [Cu2+] after 24 h							
	25 nm ENP		50 nm ENP		100 nm ENP		400 nm ENP	
	Measured	Calculated	Measured	Calculated	Measured	Calculated	Measured	Calculated
ppm/ µM	µM	µM	µM	µM	µM	µM	µM	µM
0.00/ 0.00	0.00	0.00	0.00	0.00	0.00	0.00	0.00	0.00
0.25/ 3.93	NA	2.32	NA	1.08	NA	1.02	NA	0.57
0.50/ 7.87	NA	4.41	NA	2.20	NA	2.06	NA	1.08
1.00/ 15.74	6.61	7.03	3.62	3.87	3.78	3.83	2.20	2.06
2.00/ 31.47	9.76	9.68	5.98	5.94	6.45	6.50	3.78	3.88
4.00/ 62.95	NA	11.80	NA	7.98	NA	9.85	NA	7.00
8.00/ 125.89	13.22	13.22	9.60	9.60	13.22	13.21	11.80	11.80

III. Toxicokinetic model for perivitelline Cu

To describe the toxicokinetics of the system, we assume a simple diffusion mechanism for relating the dissolved Cu concentration in the medium and that in the perivitelline space, C. Then, with k_u and k_e as the rate parameter for uptake and elimination, respectively,

$$\frac{dC}{dt} = k_u C_w(t) - k_e C(t) \tag{SI.3}$$

Under (hypothetical) constant conditions, the perivitelline concentration, C, would eventually approach a notional equilibrium value, $C^* = k_u C_w^* / k_e$, in which the ratio of parameters k_u / k_e is known as the bioconcentration factor. We use the bioconcentration factor to "scale" Equation SI.3 to a form that is particularly useful where information about Cu accumulation is scant or missing. "Scaling" is a technique for reducing an equation or system of equations to a simpler form by choosing units (i.e. "scales") for variables that take account of some of the processes being studied. It recognizes that the dynamics of biological systems are independent of the units used by scientists to make measurements. Its rationale is similar to that for "nondimensionalization" - i.e. the reduction of a dynamical system to a form where all variables and parameters are pure numbers [4, 5] – though the purpose of scaling here is to change rather than to remove the units of a variable. We define the "scaled perivitelline Cu concentration" as

$$c(t) \equiv \frac{k_e}{k_u} C(t) \tag{SI.4}$$

This scaled measure can be interpreted as the environmental dissolved Cu concentration that would be needed to get a particular (unscaled) equilibrium concentration of dissolved Cu in the perivitelline space. Rewritten in terms of c, Equation SI.3 becomes

$$\frac{dc}{dt} = \left(\frac{k_e}{k_u}\right)\frac{dC}{dt} = \left(\frac{k_e}{k_u}\right)\left(k_u C_w(t) - k_e C(t)\right) = k_e C_w(t) - k_e c(t) \tag{SI.5}$$

The general solution of the differential equation is

$$c = k_e e^{-k_e t} \int C_w(t) e^{k_e t} dt + \mathrm{A} e^{-k_e t} \tag{SI.6}$$

in which A is an integration constant.

In our experiments, $C_w(t)$ varies over time. Assuming a constant nominal ENP concentration and a negligible initial perivitelline dissolved Cu concentration, substitution of Equation SI.1 into SI.6 yields

$$c(t)=\begin{cases} 0 & t\le 4 \\ C_{nom}\left(p_2+p_1\left(\frac{1}{k_e}+t-4\right)-\left(p_2+\frac{p_1}{k_e}\right)e^{-k_e(t-4)}\right) & t>4 \end{cases} \quad \text{(SI.7)}$$

In the Hua experiments, C_w is approximately constant after initial exposure at 24 hpf. Then, evaluating the integral in Equation SI.6 yields

$$c=\begin{cases} 0 & t\le 24 \\ C_w\left(1-e^{-k_e(t-24)}\right) & t>24 \end{cases} \quad \text{(SI.8)}$$

IV. Hatching enzyme inhibition model

Cu ions shed from CuO ENPs inhibit the activity of hatching enzyme ZHE1; CuO ENPs do not affect ZHE1 activity directly [1]. The activity of *rec* ZHE1 is constant when excess substrate is available and dissolved Cu concentrations exceed those of enzyme [1], which shows that Cu^{2+} reversibly binds to ZHE1. This indicates that a classic inhibition model could describe the kinetics of ZHE1 with Cu^{2+} as inhibitor.

In its most general form, classic inhibition model describes "partial mixed competitive inhibition" kinetics, which, with a potentially variable inhibitor (i.e. dissolved Cu) concentration and constant substrate (i.e. chorion) concentration, is [6]

$$V(t)=\frac{V_{\max}+\frac{C(t)}{C_k}V^i_{\max}}{\frac{1}{s}\left(1+\frac{C(t)}{pC_k}\right)+1+\frac{C(t)}{C_k}} \quad \text{(SI.9)}$$

in which $V(t)$ is the enzymatic velocity; $V_{\max}$ is the maximum enzymatic velocity at saturating substrate concentrations; $V^i_{\max}$ is the maximum enzymatic velocity at saturating substrate and inhibitor concentrations (i.e. maximally inhibited enzymes may show activity); s is the ratio of the substrate concentration and half saturation constant (commonly denoted as 'K_m'); C_k and

pC_k are constants specifying the strength of the inhibitor. At saturating substrate concentrations, i.e. $1/s \to 0$, Equation SI.7 reduces to

$$V(t) \approx \frac{C_k V_{\max} + C(t) V^i_{\max}}{C_k + C(t)} \tag{SI.10}$$

Figure SI-2 shows that this function adequately represents the inhibitory effect of Cu^{2+} up to a least 160 μM with $V^i_{\max} = 0$ and $C_k = 41.9\,\mu M$ (95% confidence interval: 28.0 – 63.5 μM).

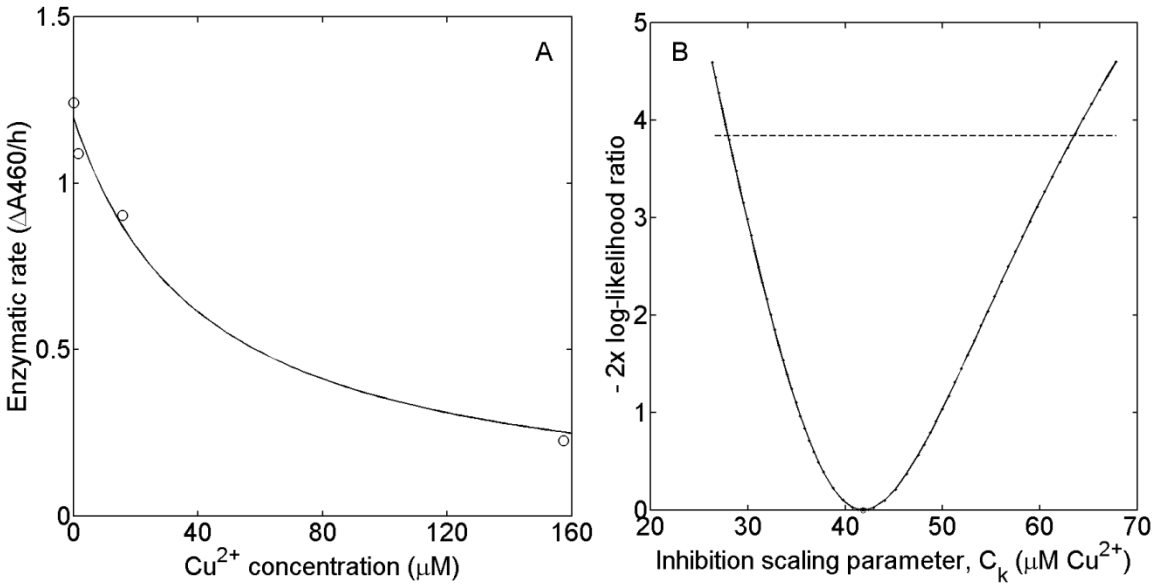

Figure SI-2. Analysis of *in vitro rec* ZHE1 activity with excess substrate and Cu^{2+} as an inhibitor. Measured enzymatic rates (data from Lin *et al.* [1]) are fitted with Equation SI-8 with $V^i_{\max} = 0$ and estimated parameters $C_k = 41.9\,\mu M$ and $V_{\max} = 1.20\,\Delta A460\ h^{-1}$ (a). The negative log likelihood profile for C_k is nearly symmetrical at its minimum with a 95% confidence interval from 28.0 to 63.5 μM, as marked by the broken line (b).

V. Hatching and toxicodynamics model

In the context of this work, a survivor is defined as an unhatched egg with a viable embryo and hazard refers to the risk of hatching or dying. Assuming that hatching and death are independent events with associated hazard rates $h_D(t)$ and $h_\dagger(t)$, respectively, the probability that an egg neither hatches nor dies, $S(t)$, changes at a rate according to

$$\frac{dS}{dt} = -S(t)\left(h_D(t) + h_\dagger(t)\right) \tag{SI.11}$$

Hence, the survivor function for unhatched viable eggs is (assuming that at the time of egg fertilization, t_0, $S(0) = 1$)

$$S(t) = e^{-\int_0^t \left(h_D(\tau)+h_\dagger(\tau)\right)d\tau} = S_\dagger(t)e^{-\int_0^t h_D(\tau)d\tau} \tag{SI.12}$$

in which $S_\dagger(t) \equiv e^{-\int_0^t h_\dagger(\tau)d\tau}$ denotes embryo survival to time *t* (we do not model embryo survival as a process here; instead, we use census data to specify $S_\dagger(t)$).

Hatching occurs when proteolytic enzymes have sufficiently damaged the chorion for the embryo to rupture it by mechanical force. We assume that all proteolytic enzymes are released in the perivitelline space at time t_r and remain fully active at least until hatching; the perivitelline space is considered to have a constant volume. Furthermore, we assume that the gain in larval strength during chorion digestion is negligible and that in absence of toxicants chorion digestion proceeds at a constant rate (i.e. the decrease in the density of enzyme attack sites during chorion digestion is negligible). Then, the total amount of digested chorion protein, $D(t)$, is

$$D(t) = \begin{cases} 0 & t \le t_r \\ \int_{t_r}^{t} V(\tau)d\tau & t > t_r \end{cases} \tag{SI.13}$$

We further assume that the probability of hatching, and thus the hazard rate associated with hatching, increases linearly with the amount of digested chorion accumulated since t_r,

$$h_D(t) = kD(t) \tag{SI.14}$$

in which k is a rate constant. Substitution of Equation SI.14 into SI.13 yields

$$h_D(t) = \begin{cases} 0 & t \le t_r \\ k\int_{t_r}^{t} V(\tau)d\tau & t > t_r \end{cases} \tag{SI.15}$$

We assume *ad libitum* substrate availability for ZHE1, which appears reasonable as the chorion is only partially digested at hatching, Substitution of Equation SI.8 (with $V_{\max}^i = 0$) into SI.15 yields

$$h_D(t) = \begin{cases} 0 & t \le t_r \\ kV_{\max} \int_{t_r}^{t} \dfrac{C_k}{C_k + C(\tau)} d\tau & t > t_r \end{cases} \quad \text{(SI.16)}$$

Scaling dissolved perivitelline Cu concentrations as before, i.e. $c(t) \equiv k_e C(t)/k_u$, and with $c_k \equiv k_e C_k / k_u$ as the scaled dissolved Cu concentration in the perivitelline space at which ZHE1 activity is halved, we get

$$h_D(t) = \begin{cases} 0 & t \le t_r \\ k_0^{'} \int_{t_r}^{t} \dfrac{c_k}{c_k + c(\tau)} d\tau & t > t_r \end{cases} \quad \text{(SI.17)}$$

in which $k_0^{'} \equiv kV_{\max}$ specifies how fast the hatching process accelerates with increasing chorion digestion in absence of Cu. Substitution of Equation into SI.12 completes the hatching model

$$S(t) = \begin{cases} S_{\dagger}(t) & t \le t_r \\ S_{\dagger}(t) e^{-k_0^{'} c_k \int_{t_r}^{t} \int_{\tau_r}^{\tau} \frac{1}{c_k + c(\omega)} d\omega d\tau} & t > t_r \end{cases} \quad \text{(SI.18)}$$

Note that in absence of ZHE1 inhibition, the integral in Equation SI.16 can be evaluated. This yields, for $t > t_r$, the Weibull distribution

$$S(t) = S_{\dagger} e^{-0.5 k_0^{'} (t - t_r)^2} \quad \text{(SI.19)}$$

VI. Hatching dynamics with no-effect concentration

To examine whether there is a significant threshold concentration of dissolved Cu in the perivitelline space below which ZHE1 inhibition does not occur, the no-effect concentration, c_0, can be estimated by substituting $\left(c(t) - c_0\right)_+$ for $c(t)$ in Equation SI.18.

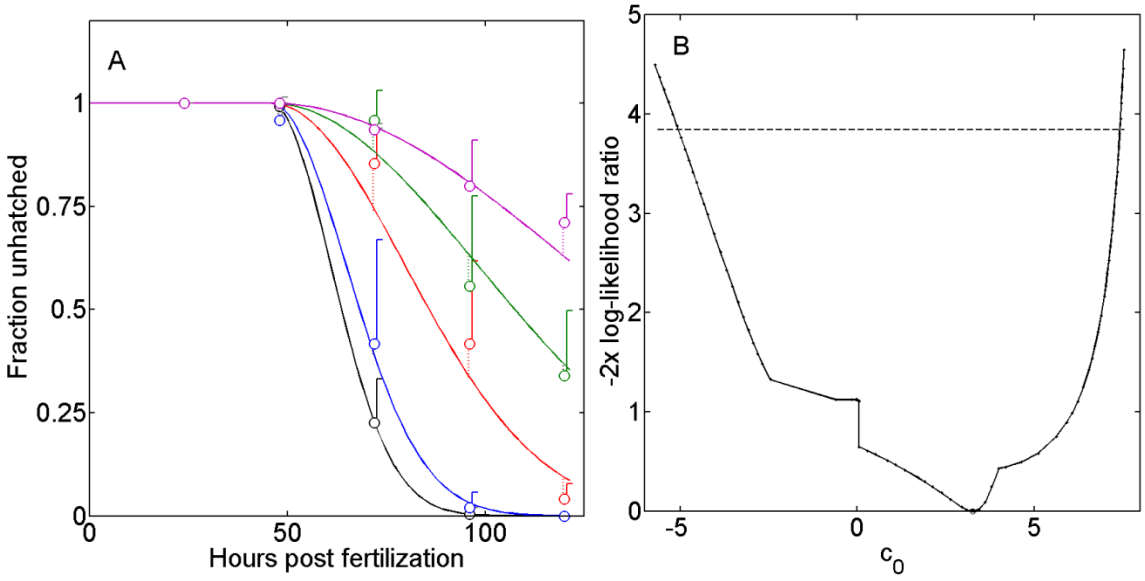

Figure SI-3. Course of the mean fraction of unhatched viable eggs exposed to $Cu(NO3)_2$ with model fits assuming a non-zero value for the scaled no-effect concentration, c_0, i.e. the threshold scaled perivitelline Cu concentration below which hatching is not impaired (A) and the corresponding negative likelihood profile for c_0 with the broken line marking the 95% confidence interval (B). From bottom to top in Panel A, curves represent model fits to data relating to nominal Cu concentrations increasing from 0 (black), 0.25 (blue), 0.5 (red), 1 (green) and 2 (purple) ppm; until approximately 50 hpf data and model fits at all exposure levels are overlapping (available data from 4 and 8 ppm CuO are excluded, as nearly all embryos died before hatching). Model fits are based on dissolved Cu concentrations in the medium and perivitelline space (with Equation 1 and 3; see main text). Dotted lines connect data to corresponding model fits. Vertical lines represent standard deviations of 15 (control) or 3 (all exposure levels) replicates of the means of 16 eggs; the mean absolute error of model predictions is 0.04. Parameter estimates are listed in Table 1. Parameter estimates are $k_0^{'} = 4.29\ 10^{-3}\ h^{-2}$; $t_r = 45.66$ h; $k_e = 0.39\ h^{-1}$ and $c_0 = 3.27$ µM. The likelihood profile in panel B shows that c_0 doesn't differ significantly from 0 at the 95% confidence level. Data from Hua *et al.* [2].

References

1. Lin, S. J.; Zhao, Y.; Ji, Z. X.; Ear, J.; Chang, C. H.; Zhang, H. Y.; Low-Kam, C.; Yamada, K.; Meng, H.; Wang, X.; Liu, R.; Pokhrel, S.; Madler, L.; Damoiseaux, R.; Xia, T.; Godwin, H. A.; Lin, S.; Nel, A. E., Zebrafish High-Throughput Screening to Study the Impact of Dissolvable Metal Oxide Nanoparticles on the Hatching Enzyme, ZHE1. *Small* **2013,** *9*, (9-10), 1776-1785.
2. Hua, J.; Vijver, M. G.; Ahmad, F.; Richardson, M. K.; Peijnenburg, W., Toxicity of different-sized copper nano- and submicron particles and their shed copper ions to zebrafish embryos. *Environmental Toxicology and Chemistry* **2014,** *33*, (8), 1774-1782.

3. Adeleye, A. S.; Conway, J. R.; Perez, T.; Rutten, P.; Keller, A. A., Influence of Extracellular Polymeric Substances on the Long-Term Fate, Dissolution, and Speciation of Copper-Based Nanoparticles. *Environmental Science & Technology* **2014,** *48*, (21), 12561-12568.
4. Nisbet, R. M., Nondimensionalization. In *Encyclopedia of Theoretical Ecology* Hastings and Gross, L. A., Ed. University of California Press: 2012.
5. Gurney, W. S. C.; Nisbet, R. M., *Ecological Dynamics*. Oxford University Press: New York, 1998.
6. Anonymous, ChemWiki: The Dynamic Chemistry E-textbook. In *Michaelis-Menten Kinetics and Briggs-Haldane Kinetics*, Larsen, D., Ed. University of California, Davis: 2015.